Vol 4 (3) (2023)

Measurement, Control, and Automation

Website: https:// mca-journal.org

ISSN 1859-0551

ZV Shaper - ADRC Combination Control for Crane System with Constrained Control Signal

Tran Thanh Bao[1], Nguyen Minh Duc[1], Duong Minh Duc[1], Do Trong Hieu[1,*]

[1]*Hanoi University of Science and Technology*

*****Corresponding author's E-mail: hieu.dotrong@hust.edu.vn*

Abstract

Gantry cranes are widely employed in various industries, including manufacturing and transportation. However, when used, the crane causes undesired cargo vibration, making it difficult to operate and workplace safety. Numerous crane control systems exist, but most are rather complex in controller design and practical implementation. Because of its ease of tuning, quick reaction, and robustness against changing process parameters, Active Disturbance Rejection Control (ADRC) is a viable alternative to standard Proportional-Integral-Derivative (PID) controllers. However, in many flexible systems, ADRC controllers have little ability to decrease residual oscillation. The input shaping method, a commonly used feedforward control strategy for vibration suppression, can be implemented to address this issue. This paper proposed a hybrid controller that combines ADRC with input shaping to achieve accurate position control, low residual oscillation in the crane system. The condition of the controller parameter is given to ensure the input signal limits.

***Keywords**: ADRC; Input shaping; limited control signal; gantry crane control*

Abbreviations

ADRC	Active Disturbance Rejection Control
PID	Proportional-Integral-Derivative
IS	Input Shaping
ESO	Extended State Observer
ZV	Zero Vibration

1. Introduction

This article discusses the challenges of operating crane systems, with a focus on controlling position and suppressing residual oscillations. Due to vibrations and residual oscillations, these systems often have significant response times, making it essential to develop effective control methods. Traditional closed-loop control methods have limitations, including difficulty identifying specific noise components and accurate modeling. They also require high-precision sensors and accurate object models, making them less suitable for crane systems.

In contrast, open-loop feedforward control methods are more commonly used and effective in controlling and suppressing residual oscillations. These methods do not rely on precise sensors or accurate object models, making them more practical for crane systems. Over the past decades, various vibration suppression control approaches have been studied, including open-loop control (input shaping [1], hybrid control [2]), closed-loop control (linear control, optimal control, adaptive control [3]) , and intelligent control (fuzzy control, neural networks, genetic algorithms [4].

In recent years, Active Disturbance Rejection Control (ADRC) has been considered to replace the traditional PID controller. The concept of ADRC was proposed by J. Han[5], but only became explicit for the application of this method since a controller parameter tuning method was proposed in ADRC is a powerful control method in which system models are extended with a new state variable, including all unknown dynamics and disturbances. According to the studies [6,7], in crane control, the ADRC method is more effective than the PID control method in reducing the swing angle of the system, the ADRC method is also capable of compensating for nonlinear properties of the motor system such as dead-zone and input saturation. This makes it a more powerful and flexible control method than the PID controller, especially in applications with external disturbances.

Previous studies have given limited consideration to the constraint of control signals. If they have utilized input-shaping in conjunction with PID controllers, they have not addressed the ADRC controller. ADRC can estimate and suppress external disturbances while minimizing errors and improving control system performance. When combined with Input Shaping, ADRC becomes more effective in suppressing vibrations and improving performance. This article proposes combining ADRC and Input Shaping controllers to control the

Received: 5 July 2023; Accepted: 8 September 2023.

crane position while suppressing residual oscillations with limited control signals.
The article is organized as follows: Section 2 presents the mathematical model of the crane system. Section 3 discusses the design of position control and vibration suppression using ADRC and input shaping. Simulation results are described in Section 4 to demonstrate the effectiveness of the proposed approach. Section 5 concludes the article by summarizing key findings and potential future research directions.

2. Dynamic model of Crane system

Considering the model of an overhead crane system moving horizontally along the X- axis, with a payload hanging below along the Y-axis as shown in Figure 1, where:

- *x:* position of the trolley along the X-axis
- *l:* length of the hoisting cable
- θ*:* sway angle
- m_p: mass of the trolley
- m_t: mass of the payload

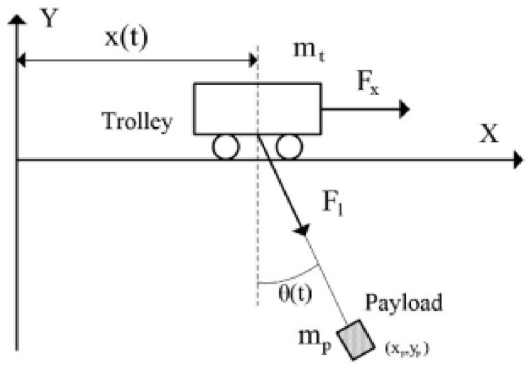

Figure 1: An overhead crane system

Basically, both the trolley and the payload are considered as point masses, and the friction between the trolley and the rail is neglected. Suppose that the tension force that will cause the hoisting cable to elongate is neglected, the equations for the gantry crane model are:

$$(m_t + m_p)\ddot{x} + m_p l\ddot{\theta}\cos\theta - m_p l\dot{\theta}^2 \sin\theta = F_x - B_{eq}\dot{x} \quad (1)$$

$$l\ddot{\theta} + \ddot{x}\cos\theta + g\sin\theta = -B_p\dot{\theta} \quad (2)$$

where:
F_x : the force drives the system
B_{eq} : the viscosity index
B_p : the damping coefficient

From equation (1), one has the form:

$$\ddot{x} = \frac{-m_p}{m_p + m_t}\left[\left(l\ddot{\theta}\cos\theta - l\dot{\theta}^2\sin\theta\right) - B_{eq}\dot{x}\right] + \frac{F_x}{m_p + m_t}$$

In practice, the trolley is moved by using a motor and motor driver, allowing for precise speed control even in the presence of disturbances. As a result, it is reasonable to assume that the trolley velocity can be managed by adjusting the input voltage. The transfer function for the trolley position in response to a control voltage input can be consider as [8]:

$$G_P = \frac{X(s)}{U(s)} = \frac{K}{(Ts+1)s} \quad (3)$$

where $K > 0, T > 0$

From equation (2), when the angle of oscillation is small, $cos\theta \approx 1, sin\theta \approx \theta$, we consider that there is a transfer function between the angle of oscillation and the position:

$$\frac{\theta(s)}{X(s)} = \frac{-s^2}{ls^2 + B_p s + g} \quad (4)$$

where: $B_p = 2\xi\sqrt{gl}$ and ξ is the damping coefficient.

3. Control system design

In this paper, we proposed the combination of ADRC with 2-pulse input shaping (called ZV shaper) to control crane, where ADRC controls the trolley position and the ZV Shaper is responsible for reducing oscillations and suppressing residual oscillations of the payload.

This control structure is shown in Figure 2 where ADRC controls the crane position and the ZV Shaper is responsible for reducing oscillations and suppressing residual oscillations of the payload.

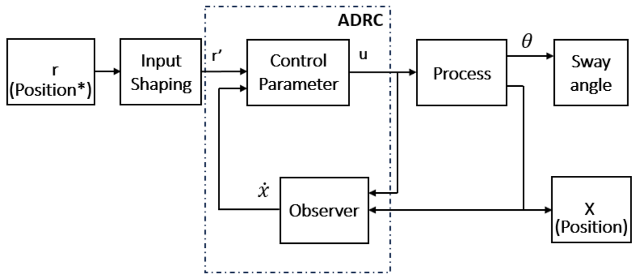

Figure 2: Control System Structure

3.1. *Input Shaping*

Input shaping is an input filter used to eliminate residual oscillations of the system. The idea of this technique is to eliminate the response of the previous pulse by issuing subsequent pulses at an appropriate time with an appropriate magnitude. At this point, the response of the subsequent pulse will eliminate part of the response of the previous pulse. So, until the last pulse is applied, the residual oscillation of the system will be eliminated.

Consider an oscillating system represented as a second-order function as follows:

$$\frac{X(s)}{F(s)} = \frac{\omega_0^2}{s^2 + 2\xi\omega_0 s + {\omega_0}^2} \quad (5)$$

where:

ω_0 : the natural frequency of the system
ξ : the damping ratio

If an input pulse with magnitude A_I is applied to the system at time t_I, then the output response $y(t)$ is determined:

$$y(t) = B_1.sin(\omega.t + \theta_1) \quad (6)$$

where:

$$B_1 = A_1.\frac{\omega_0}{\sqrt{1-\xi^2}}e^{-\xi\omega(t-t_1)},$$

$$\omega = \omega_0\sqrt{1-\xi^2}\text{ , and } \quad \theta_1 = \omega_0\sqrt{1-\xi^2}t_I$$

As mentioned above, after the first pulse has been emitted, we emit a second pulse; the output response of the two pulses is calculated as follows:

$$y(t)=B_1.\sin(\omega.t+\theta_1)+B_2.\sin(\omega.t+\theta_2) \quad (7)$$

Trigonometric transformation obtained:

$$y(t) = B_0.\sin(\omega.t + \theta_0) \quad (8)$$

with:

$$B_0 = \sqrt{(B_1.sin\theta_1 + B_2.sin\theta_2)^2 + (B_1.cos\theta_1 + B_2.cos\theta_2)^2}$$

$$\theta_0 = tan^{-1}(\frac{B_1.sin\theta_1 + B_2.sin\theta_2}{B_1.cos\theta_1 + B_2.cos\theta_2})$$

In the general case, if we apply N pulses to amplitude A_i at time t_i $(i=1,......, N)$, then the response of N pulses is determined by:

$$y(t) = \sum_{i=1}^{N} y_i(t) \sum_{i=1}^{N} B_i.sin(\omega.t + \theta_i) \quad (9)$$

with:

$$B = \sqrt{\left(\sum_{i=1}^{N} B_i.sin(\theta_i)\right)^2 + \left(\sum_{i=1}^{N} B_i.cos(\theta_i)\right)^2}$$

$$\theta = tan^{-1}(\frac{\sum_{i=1}^{N} B_i.sin(\theta_i)}{\sum_{i=1}^{N} B_i.cos(\theta_i)})$$

In this paper, the input shaping method is considered with 2-pulse, called ZV (Zero Vibration) shaper, corresponding to $N = 2$, with magnitude A_1 and A_2 at time instant t_1 and t_2 respectively, these parameters are determined as follows:

$$\begin{cases} A_1 = \dfrac{1}{1+K^*}, & t_1 = 0 \\ A_2 = \dfrac{K^*}{1+K^*}, & t_2 = \dfrac{\pi}{\omega_d} \end{cases} \quad (10)$$

where:

$$K^* = exp\left(-\frac{\pi\xi}{\sqrt{1-\xi^2}}\right);\ \omega_d = \omega_0\sqrt{1-\xi^2}$$

3.2. *ADRC for trolley position control*

To construct the ADRC controller for the trolley position control, transform equation (3) into the form:

$$\ddot{x} = f + b_0.u \quad (11)$$

with:

$$f(t) = \frac{-1}{T}\dot{x} \text{ and } b_0 = \frac{K}{T}$$

An Extended State Observer (ESO) is constructed to estimate the value of f, thereby compensating for the impact of f on the model using disturbance rejection method. The extended observer is designed in the form of:

$$\begin{cases} \dot{\hat{x}}_1(t) = \hat{x}_2(t) + l_1(y(t) - \hat{x}_1(t)) \\ \dot{\hat{x}}_2(t) = \hat{x}_3(t) + b_0.u(t) + l_2(y(t) - \hat{x}_1(t)) \\ \dot{\hat{x}}_3(t) = l_3(y(t) - \hat{x}_1(t)) \end{cases} \quad (12)$$

where, l_1, l_2, l_3 are observer parameters to be determined such that $\hat{x}_1, \hat{x}_2, \hat{x}_3$ will track $x, \dot{x}, f$.

Then, with the control law of the form: $u = (u_0 - \hat{x}_3)/b_0$ Equation (9) will be converted to the form of two simple integration stages:

$$\ddot{x}(t) = u_0 \quad (13)$$

One of the simple proposed ways to choose a control law is to choose:

$$u_0 = K_P(r - \hat{x}_1) - K_D.\hat{x}_2 \quad (14)$$

Substituting (14) into (13):

$$\ddot{x}(t) = K_P\big(r(t) - x(t)\big) - K_D.\dot{x}(t) \quad (15)$$

The closed-loop transfer function of the position control loop is then:

$$G_{cl}(s) = \frac{X(s)}{R(s)} = \frac{K_P}{s^2+K_Ds+K_P} \quad (16)$$

where K_P and K_D are the parameters of the controller.

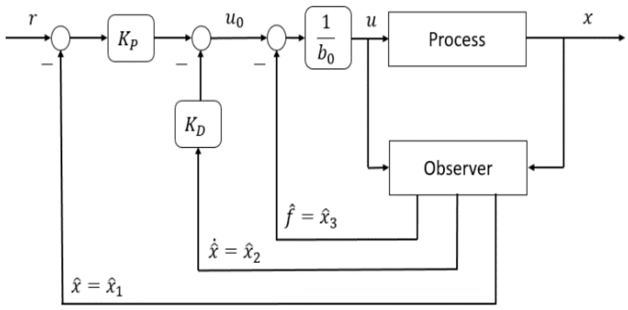

Figure 3: ADRC for a second-order plant

These parameters, along with the parameters of the extended observer, can be selected according to the method proposed by [9], where T_{set} is the desired settling time of the closed-loop response.

$$\begin{cases} K_P = (s^{CL})^2, K_D = -2s^{CL}, \\ l_1 = -3.s^{ESO}, l_2 = 3(s^{ESO})^2, l_3 = (s^{ESO})^3 \\ s^{CL} \approx -\dfrac{5.85}{T_{set}}, s^{ESO} = (3 \ldots 10)s^{CL} \end{cases} \quad (17)$$

where

s^{CL} : the closed loop pole

s^{ESO} : the observer pole

Then the transfer function of the closed-loop position control loop:

$$G_{cl}(s) = \frac{X(s)}{R(s)} = \frac{(s^{CL})^2}{(s-s^{CL})^2} \quad (18)$$

3.3. *Control signal examination*

In this article, we consider the case that the control signal is limited to a certain range of values, that is:

$$V_{min} \le u(t) \le V_{max} \quad (19)$$

This condition will lead to some constraints on the parameter of the controller.

3.3.1. In the case without ZV shaper

Let $a = -s^{CL} (a > 0)$, equation (18) takes the form:

$$G_{cl}(s) = \frac{X(s)}{R(s)} = \frac{a^2}{(s+a)^2} \quad (20)$$

The transfer function of the controller output response can be obtained through:

$$\frac{U(s)}{R(s)} = \frac{U(s)}{X(s)}.\frac{X(s)}{R(s)} = \frac{1}{\frac{X(s)}{U(s)}}.G_{cl}(s) \quad (21)$$

with $\frac{X(s)}{U(s)}$ is the transfer function between the position output and control signal, $\frac{X(s)}{R(s)}$ is the closed – loop transfer function of the trolley position control.

Let $r(t) = L\delta(t), (L > 0)$ or $R(s) = \frac{L}{s}$ then:

$$U(s) = \frac{R(s)}{\frac{X(s)}{U(s)}}.\frac{X(s)}{R(s)} = L.\frac{(Ts+1)}{K}.\frac{a^2}{(s+a)^2} \quad (22)$$

Taking the inverse Laplace transform of *U(s):*

$$u(t) = \frac{L.a^2}{K}.[T.e^{-at} - (T.a-1).t.e^{-at}] \quad (23)$$

To find local maximum/minimum of *u(t),* we solve following equation:

$$u'(t) = \frac{L.a^2}{K}.e^{-at}[1 - 2.a.T + a.(a.T-1)t] = 0 \quad (24)$$

The local maximum/minimum of *u(t)* is determined at the time

$$t_m = \frac{2aT-1}{a(aT-1)}$$

Then: $$u(t_m) = \frac{L.a}{K}.(1-aT).e^{\frac{1-2aT}{aT-1}} \quad (25)$$

Case 1: *if* $a \in (0; \frac{1}{2T}]$

Then $t_m > 0$ and $\begin{cases} u'(t) > 0 \; when \; 0 < t < t_m \\ u'(t) < 0 \; when \; t_m < t < \infty \end{cases}$

From equation (25):

$$u(t_m) = \frac{L.a}{K}.(1-aT).e^{\frac{1-2aT}{aT-1}} = u(t)_{max} \quad (26)$$

Combined with the limit condition (19), the following condition must be satisfied:

$$0 < u(t)_{max} = \frac{L.a}{K}.(1-aT).e^{\frac{1-2aT}{aT-1}} \le V_{max} \quad (27)$$

Case 2: *if* $a \in (\frac{1}{T}; +\infty)$

Then $t_m > 0$ and $\begin{cases} u'(t) < 0 \; when \; 0 < t < t_m \\ u'(t) > 0 \; when \; t_m < t < \infty \end{cases}$

We have:

$$u(t_m) = \frac{L.a}{K}.(1-aT).e^{\frac{1-2aT}{aT-1}} = u(t)_{min} < 0 \quad (28)$$

The solution set of a in this case is obtained with the following conditions:

$$\begin{cases} u(0) = \frac{L.a^2}{K}.T \le V_{max} \\ V_{min} \le u(t)_{min} = \frac{L.a}{K}.(1-aT).e^{\frac{1-2aT}{aT-1}} < 0 \end{cases} \quad (29)$$

Case 3: *if* $a \in (\frac{1}{2T}; \frac{1}{T}]$

In this case, $t_m < 0$ and $u'(t) < 0 \; \forall t \ge 0$, thus obtaining the following conclusion:

$$u(t)_{max} = u(0) = \frac{L.a^2}{K}.T \le V_{max} \quad (30)$$

From conclusions (27), (29), and (30), we can derive a comprehensive result about the conditions for the value of a such that the condition in equation (19) is satisfied. It will belong to one of the following conditions:

$$(I) \begin{cases} a \in (0; \frac{1}{2T}] \\ \frac{L.a}{K}.(1-aT).e^{\frac{1-2aT}{aT-1}} \le V_{max} \end{cases} \quad (31)$$

$$(II) \begin{cases} a \in (\frac{1}{T}; +\infty) \\ \frac{L.a^2}{K}.T \le V_{max} \\ V_{min} \le \frac{L.a}{K}.(1-aT).e^{\frac{1-2aT}{aT-1}} < 0 \end{cases} \quad (32)$$

$$(III) \begin{cases} a \in (\frac{1}{2T}; \frac{1}{T}] \\ \frac{L.a^2}{K}.T \le V_{max} \end{cases} \quad (33)$$

3.3.2. *In the case with ZV shaper*

The transfer function in the Laplace domain of two-pulse input shaping:

$$G_{ZV} = A_1 + A_2.e^{-s\tau}$$
$$A_1 + A_2 = 1; \quad A_1, A_2 > 0 \quad (34)$$

In this case, the transfer function of the controller output response is obtained :

$$U(s)_{ZV} = \frac{R(s)}{\frac{X(s)}{U(s)}}.G_{CL}.G_{ZV} = \frac{L.a^2}{K}.\left[A_1.\frac{Ts+1}{(s+a)^2} + A_2\cdot\frac{Ts+1}{(s+a)^2}.e^{-s\tau}\right] \quad (35)$$

Taking the inverse Laplace transform of $U(s)_{ZV}$:

$$u(t)_{ZV} = A_1.u(t) + A_2.u(t-\tau).h(t-\tau) \quad (36)$$

with $\begin{cases} h(t-\tau) = 0 \text{ when } 0 \le t < \tau \\ h(t-\tau) = 1 \text{ when } t \ge \tau \end{cases}$

Considering condition in (34), then from (36), It can be observed that in the case where the system has ZV shaper, it can always be proven that:

$$u(t)_{ZV} < u(t)_{max} \ (\forall t \ge 0) \quad (37)$$

with $u(t)_{max}$ being the maximum value of the control signal when the system input does not have ZV:

Therefore, in this case, the equations (31) to (33) become sufficient conditions to calculate and select the value of **a** such that:

$$V_{min} < u(t)_{ZV} < V_{max} \quad (38)$$

4. Simulation Result

In this section, we consider system in equation (3) with the $K = 6.14$ and $T = 0.04$. Suppose that the desire trolley position is $L = 40cm$ and the control signal is limited to a range of values [-10(V),10(V)].

Table 1: The systems parameters

Symbol	Description	Value
B_p	Equivalent viscous damping of crane seen from the rope axis.	0(Ns/rad)
ω_0	System natural frequency	4.04(rad/s)
l	Rope length	0.6 (m)
A_1	Magnitude of the first pulse	0.5
A_2	Magnitude of the second pulse	0.5
t_1	Time instant of the first pulse	0 (s)
t_2	Time instant of the second pulse	0.776 (s)

With the above system parameters, the value of $\boldsymbol{a}$ is only satisfied with the condition in **case I** (equation (31)), and the specific solution range of $\boldsymbol{a}$ is determined as follows:

$$\boldsymbol{a} \in (\mathbf{0; 4.1}] \quad (39)$$

To verify the performance of proposed controller, we will examine several scenarios with $a = 1.4, a = 2.2, a = 4.2$ and $a = 15$. From Figure 4 to Figure 15, we have the results of the position response of the trolley, the sway angle of the load and the control signal in their respective cases.

Scenario 1: $\boldsymbol{a} = \mathbf{1.4}$

ADRC parameters: $K_P = a^2 = 1.96, \ K_D = 2a = 2.80$

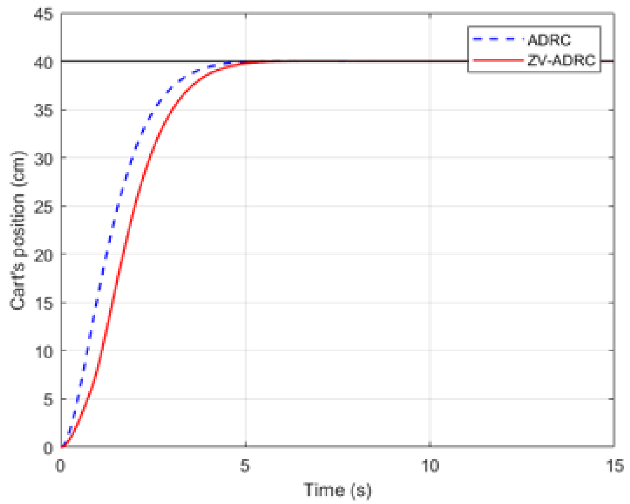

Figure 4: Trolley position with a = 1.4

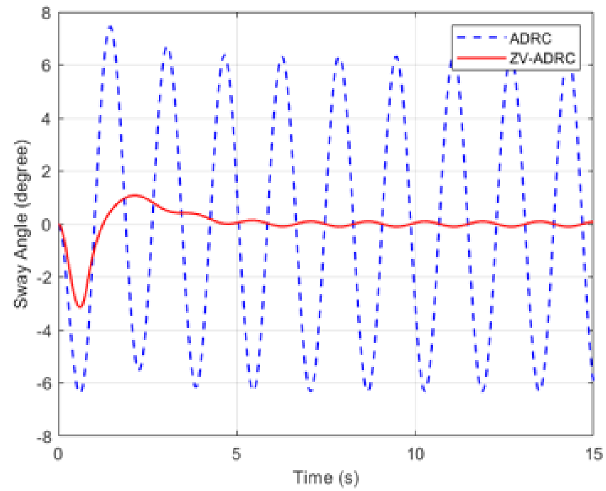

Figure 5: Payload sway angle with a = 1.4

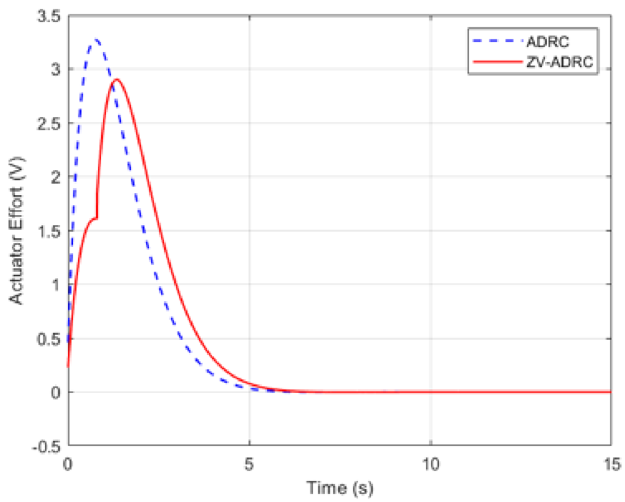

Figure 6: Control input with a = 1.4

***Scenario 2*: $\boldsymbol{a = 2.2}$**

ADRC parameters: $K_P = a^2 = 4.84, K_D = 2a = 4.40$

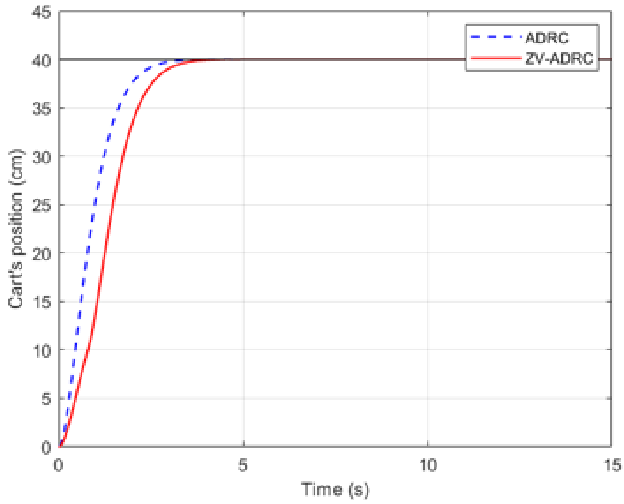

Figure 7: Trolley position with a = 2.2

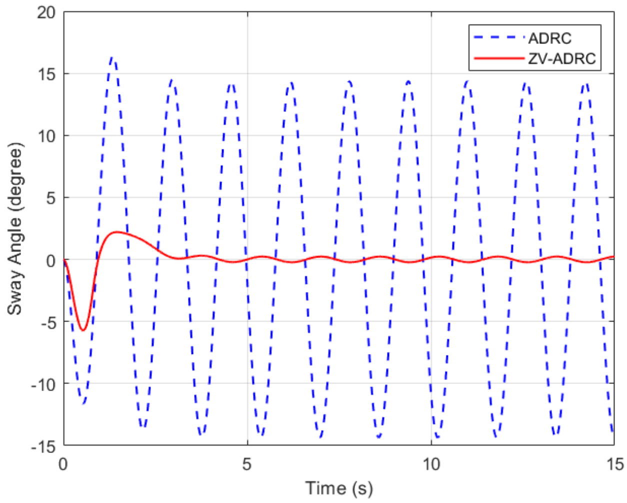

Figure 8: Payload sway angle with a = 2.2

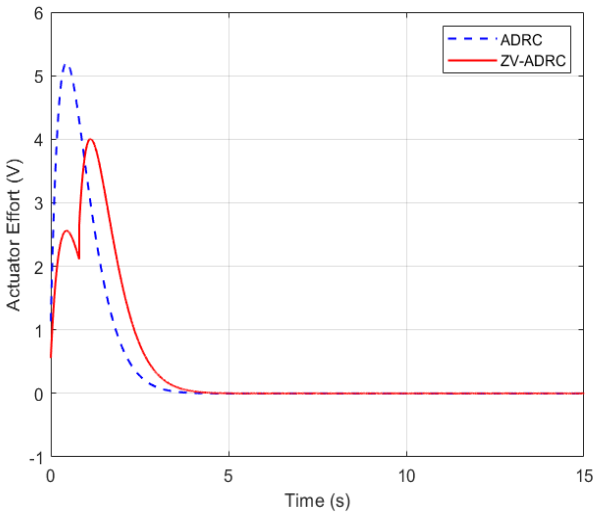

Figure 9: Control voltage with a = 2.2

***Scenario 3*: $\boldsymbol{a = 4.2}$**

ADRC parameters: $K_P = a^2 = 17.64, K_D = 2a = 8.4$

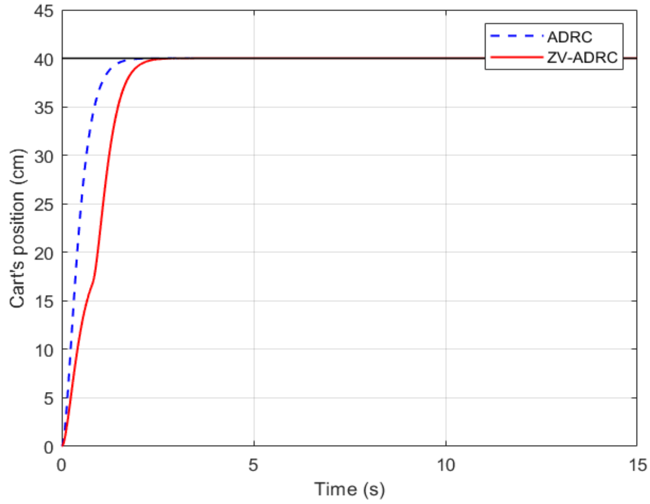

Figure 10: Trolley position with a = 4.2

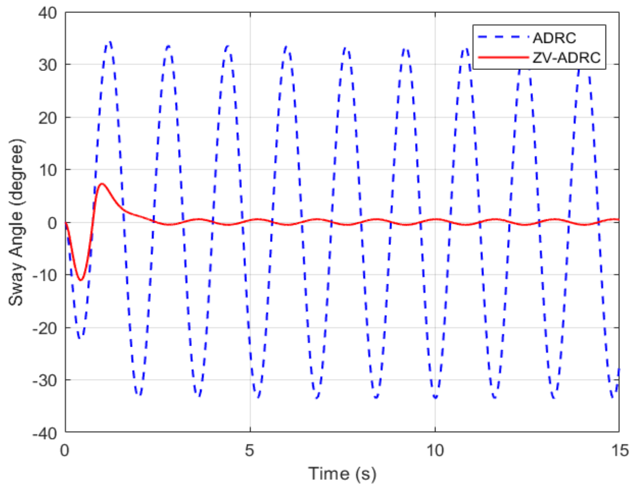

Figure 11: Payload sway angle with a = 4.2

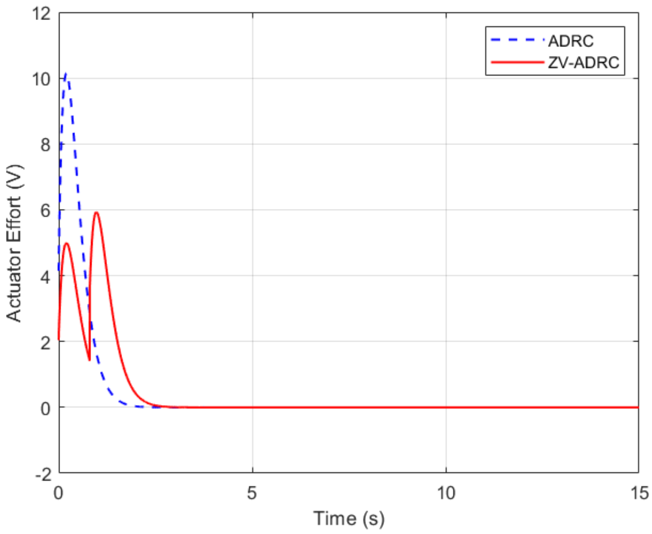

Figure 12: Control voltage with a = 4.2

***Scenario 4*: $a = 15$**

ADRC parameters: $K_P = a^2 = 225, K_D = 2a = 30$

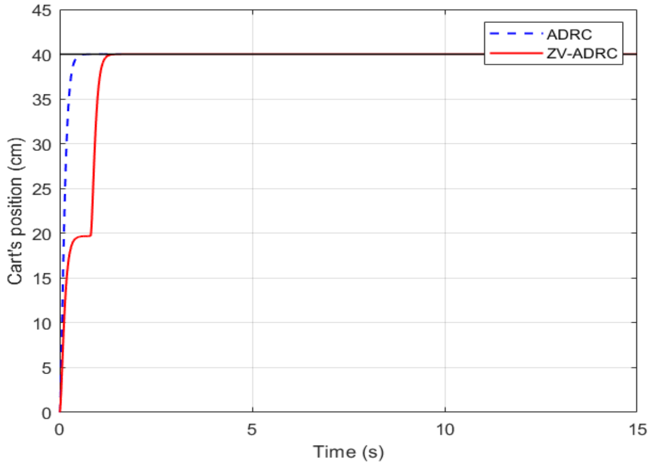

Figure 13: Trolley position with a = 15

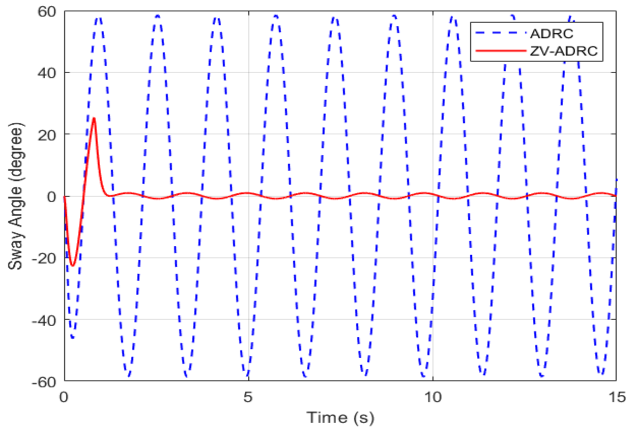

Figure 14: Payload's sway angle with a = 15

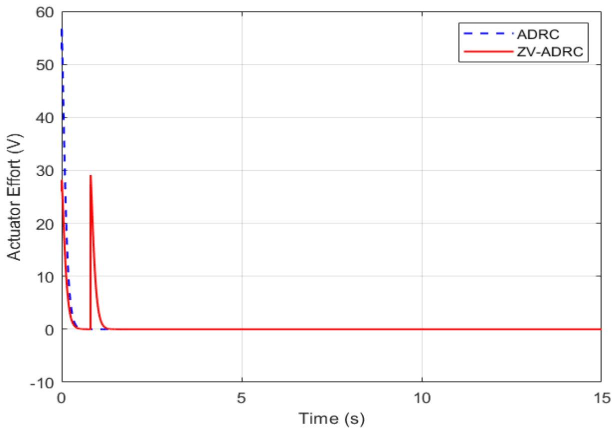

Figure 15: Control voltage with a = 15

These figures illustrate that as the value of parameter a increases, the position response time of the system improves but the sway angle of the load increases. The application of input shaping has been found effective in minimizing load oscillation. By selecting the values of a using (39), the control signal $u(t)$ meets the limit condition both with and without input shaping. For $a = 4.2$, the control signal exceeds the limit when input shaping is not considered, but it remains within the limit when an input shaping is added. This is because the conditions specified in equations (31) to (33) are only sufficient condition for the ZV-ADRC controller. In the case of $a = 15$, the Figure 15 clearly indicates that the control signal exceeds the limit region. Table 2 summarizes some reference values for each control case.

Table 2: Performance index

a		1.4	2.2	4.2	15
Residual vibration (°)	ADRC	7.45°	16.37°	34.66°	14.35°
	ZV-ADRC	3.15°	5.73°	11.07°	14.35°
Response time (s)	ADRC	3.83	2.52	1.36	0.40
	ZV-ADRC	4.35	3.08	1.98	1.15
Settling time (s)	ADRC	5.05	4.13	2.49	0.76
	ZV-ADRC	6.08	4.76	3.15	1.51
Actuator effort max (V)	ADRC	3.27	5.02	10.15	57.26
	ZV-ADRC	2.90	4.01	5.93	29.06

5. Conclusions

In this study, we have proposed the idea of combining an input shaping called ZV shaper with ADRC controller to achieve position control and reduce residual oscillation of the crane system. Under the constraint of limited control signals, we have investigated the conditions for parameter computation of the ADRC controller. Through some simulation results, it has been shown that the proposed approach not only enables the system to achieve the desired position and mitigate residual oscillations but also ensures system stability during operation.

References

[1] C. -G. Kang, "Impulse Vectors for Input-Shaping Control: A Mathematical Tool to Design and Analyze Input Shapers," in IEEE Control Systems Magazine, vol. 39, no. 4, pp. 40-55, Aug. 2019.

[2] K. Yano, K. Terashima, "Development and evaluation of operator support system for rotary crane," *18th IEEE International Conference on Control Applications,* pp. 1637-1642, 2009.

[3] E. Abdel-Rahman, A. Nayfeh, Z. Masoud, "Dynamics and control of cranes: A review," *Journal of Vibration and Control,* pp. 863-908, 2003.

[4] P. Hyla, "The crane control systems: A survey," *17th International Conference on Methods & Models in Automation & Robotics (MMAR),* pp. 505-509, 2012.

[5] Z.Gao, Y.Huang, J.Han, "An alternative paradigm for control system design," *40th IEEE Conference on Decision and Control,* pp. 4578-4585, 2001.

[6] J.Han, "From PID to active disturbance rejection control," *IEEE Trans. Ind. Electronics.,* tập 56, pp. 900-906, 2009.

[7] LIU Shu-guang, ZHANG Long, YUE Chao-qi, "An ADRC- based Positioning and Anti-swing Control for Tower Crane," *China Automation Congress (CAC),* pp. 7880-7884, 2021.

[8] Mahmud Iwan Solihin, Wahyudi Wahyudi, Ari Legowo, "Fuzzy-tuned PID Anti-swing Control of Automatic Gantry Crane," *Journal of Vibration and Control,* 2010.

[9] G. Herbs, "A Simulative Study on Active Disturbance Rejection Control as a Control Tool for Practitioners," *electronics,* pp. 246-279, 2013.

[10] D. Yoo, S. S. T. Yau, Z.Gao, "On convergence of the linear extended observer," *IEEE International Symposium on Intelligent Control,* p. 1645–1650, 2006.